Layered Graphene Transmission Line as a Tunable Band Stop Filter and Amplitude Modulator at Terahertz Frequencies

Saughar Jarchi[1*]

Abstract- In this paper, the effects of loading the substrate of a series of graphene transmission lines, in a terahertz frequency band, by longitudinal graphene strips, are investigated and numerically simulated. Two applications of a tunable band-stop filter and amplitude modulator are designed. At first, a single graphene strip is inserted in the substrate of a series transmission. It is shown that by changing the chemical potential of the inserted graphene strip, in the range of 0-0.6 eV with step of 0.2 eV, a tunable band-stop filter which supports four cases of all-pass response and 10-dB rejection bands of 1.77-2.55 THz (36.1%), 2.55-3.47 THz (30.5%) and 3.13-4.1 THz (26.8%) in the frequency range of 1-5 THz is obtained. Then, to generalize the structure to obtain more flexibility and cover a wider range of applications, three parallel longitudinal strips are placed in the substrate, and the transmission response with varying chemical potential of all the graphene strips is calculated. It is observed that, with changing chemical potential of graphene elements in the range 0-1.4 eV, a tunable band-stop filter with lower bandwidths of 1.94-2.49THz (24.8%), 3.52-3.68THz (4.4%), 4.25-4.82THz (12.56%), which is applicable for high quality systems, as well as an amplitude modulator with more than 10 cases of modulation depths ranging from 0 to 100%, in the frequency range of 3.4-3.8 THz, and with optimum performance at the frequency of 3.6 THz, are obtained.

Keywords- **Amplitude modulator, Band-stop filter, Graphene, Series transmission line, Terahertz frequency**

I. INTRODUCTION

Due to its high frequency, the terahertz frequency band provides high capacity with low-latency signal transmission and is promising for 6G communications. In recent years, with the development of THz sources, this frequency range has attracted researchers' attention, and a variety of devices for communication purposes, such as antennas, filters, switches, modulators, sensors, metasurfaces, and others, have been designed and investigated [1-6].

In the design of THz devices, in addition to conventional metals such as gold and silver, graphene is widely employed [7-11]. Graphene is a single layer of carbon atoms with a 0.34 nm thickness. In many applications, few-layer graphene (graphene with fewer than 6 layers) and multi-layer graphene (6 to 30 layers) are used. Graphene can be fabricated using several methods, including chemical vapor deposition, mechanical exfoliation, epitaxial growth, etc., and it can be produced on a variety of substrates, including Si, SiO2, Al2O3 [12], [13]. In this paper, multi-layer graphene with 10 nm thickness, approximately 30 layers, is considered.

Surface plasmon polaritons (SPP), which are surface waves propagating on the surface boundary of a metal and a dielectric in optical frequencies, can be supported by graphene at lower frequencies of infrared and THz [1]. Another special feature of graphene in the THz frequency band is its tunable conductivity, which enables the design of reconfigurable devices [14-20].

Graphene is widely applied to design THz antennas with reconfigurable properties of radiation pattern, polarization, and frequency [21]. Terahertz absorbers based on graphene and hybrid metal-graphene structures are designed and investigated [22]. Modulators in the THz frequency band for communication applications, utilizing the tunable conductivity of graphene, are proposed and studied [23]. Graphene intelligent surfaces with beam steering properties for 6th generation communications are designed and investigated [24]. Various metasurface sensors are proposed in the THz frequency band, and graphene elements in their structures are employed [25].

While a vast amount of work is performed in designing parallel structures for filter and modulator applications, there are a few published works for series configurations in the THz frequency band. Although series configurations are a basic means of realizing microwave and millimeter-wave devices such as filters, couplers, power dividers, etc., they can be employed in THz frequencies and integrated photonic devices as well [26], [27]. A series switch, based on SPP propagation, using graphene, is designed and investigated in near-infrared frequencies in [1]. The proposed structure provides two cases for the transmitted signal and implements a switch's on and off states. In reference [28], a series amplitude modulator is designed that utilizes six transverse graphene strips in the dielectric layer beneath the signal transmission line.

In this paper, a double-layer series transmission line composed of longitudinal graphene strips inserted in the substrate is investigated. It is shown that by changing the chemical potential of graphene parts, a tunable band-stop filter as well as an amplitude modulator are obtained. In the previous work of the author [28], an amplitude modulator is designed using six transverse graphene strips in the substrate. In this work, by applying longitudinal strips, two different applications of a tunable band-stop filter and amplitude modulator are achieved using a single series transmission line configuration.

1. Faculty of Technical and Engineering, Imam Khomeini International University, Qazvin, Iran.
* Email: s.jarchi@eng.ikiu.ac.ir, saugharjarchi@gmail.com

II. Theory of the designs

The series transmission line of this paper is inspired by multilayer microstrip structures. Metallic parts of conventional transmission lines are implemented by graphene; the controllable conductivity variations of graphene in the THz frequency band are utilized to fulfill the required tunable functionality. As is known from research papers, the conductivity of graphene in the THz frequency band can be stated by [29], [30]:

$$\sigma(\omega) = \frac{2e^2}{\pi\hbar}\frac{k_B T}{\hbar}\ln\left[2cosh\left[\frac{E_F}{2k_B T}\right]\right]\frac{i}{\omega + i\tau^{-1}} \quad (1)$$

Where, e represents the electron charge, T is the temperature in Kelvin, $\hbar$ stands for the reduced Planck constant, k_B shows the Boltzmann constant, τ is the relaxation time and E_F is the chemical potential or Fermi energy. The conductivity can be changed in a wide range using several methods, including an electrostatic bias voltage, a magneto-static field, chemical doping, and optical stimulation. The conductivity of graphene elements in this paper are supposed to be changed by applying an electrostatic bias voltage.

Graphene can support surface plasmon polaritons (SPP) at terahertz frequencies. Dispersion relation of SPP modes propagating on a graphene sheet surrounded by media with dielectric constants of ϵ_r1 and ϵ_r2 is calculated from [1]:

$$\frac{\omega\epsilon_{r1}\epsilon_0}{\sqrt{\epsilon_{r1}k_0^2 - k_p^2}} - \frac{\omega\epsilon_{r2}\epsilon_0}{\sqrt{\epsilon_{r2}k_0^2 - k_p^2}} = -\sigma \quad (2)$$

Where $k_p = \beta - j\alpha$ represents the propagation constant of SPPs and $k_0 = \omega/c$ is the wavenumber of free space. The dispersion relation is strongly dependent on the conductivity of graphene, σ, which is a function of chemical potential, μ_c, and relaxation time, τ. Therefore, the SPP propagation on a graphene sheet can be engineered to overcome the desired characteristics with the proper selection of μ_c and τ. However, the dispersion relation of SPP waves on graphene strips is complicated and should be exploited by numerical techniques.

III: Design and simulation results

The designed structures of this paper are based on a series of graphene transmission lines loaded by graphene elements in the substrate, which was first introduced in [28]. In the presented transmission line, graphene is employed instead of metal, due to its tunable conductivity, which provides a means of controlling electromagnetic wave propagation in the THz frequency band. In this work, to simulate graphene elements, the relaxation time is considered τ=1ps, the same value as the reference [30]. The temperature equals T=295K and the thickness of graphene is 10nm. All the simulations are performed using CST Microwave Studio software. Two different configurations, composed of a single graphene strip and three longitudinal graphene strips inserted in the substrate, are studied. In the proposed structures, the maximum value of chemical potential is considered as 1.4eV, which is reasonable according to previously published papers on graphene structures.

A. A single graphene strip inserted in the substrate

The layered series graphene transmission line is shown in Fig. 1, which the upper graphene strip, employed as the main transmission line, is placed on a SiO2 layer backed by a graphene sheet. A graphene strip is inserted in the SiO2 substrate which a distance of t=1μm from the edges of the first and second ports to prohibit electric contact with these ports. The dimensions of the structure shown in Fig. 1 are according to Table I.

TABLE I
Dimensions of the TL Illustrated in Fig. 1(a) (in μm).

Parameter	W	L	a	b	d_1	d_2	t
value	10	20	7	18	5	2	1

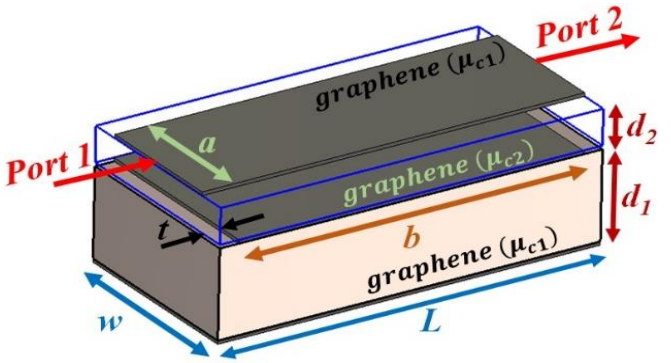

(a)

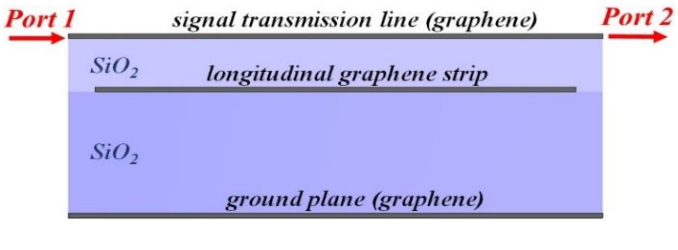

(b)

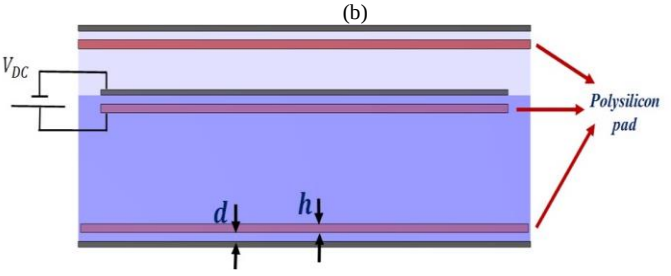

(c)

Fig. 1. Series graphene TL loaded by a single graphene strip: (a) perspective view, (b) side view, (c) biasing structure of graphene elements.

To change the chemical potential of the graphene elements, an electrostatic bias voltage is utilized [30]. Polysilicon pads with a thickness of $h = 100nm$ are inserted in the substrate with a distance of $d = 50nm$ from the graphene element and the bias voltage are applied between the polysilicon pad and the

graphene, as shown in Fig. 1(c). Chemical potential of the uppermost and the lowermost graphene elements, designated by μ_{c1} in Fig. 1, is kept constant and equal to 1.4 eV while the chemical potential of the middle graphene element, shown by μ_{c2}, is varied to provide a tunable response. Transmission of the structure, i.e., magnitude of S_{21}, is simulated and plotted in Fig. 2 for four values of μ_{c2} equal to 0, 0.2, 0.4, and 0.6 eV. The layered transmission line provides a band-stop filter with a tunable rejection band. In addition, for $\mu_{c2} = 0eV$, the input signal is directed to the output port, with a small insertion loss, and the rejection band is eliminated in the frequency range of 1-5 THz.

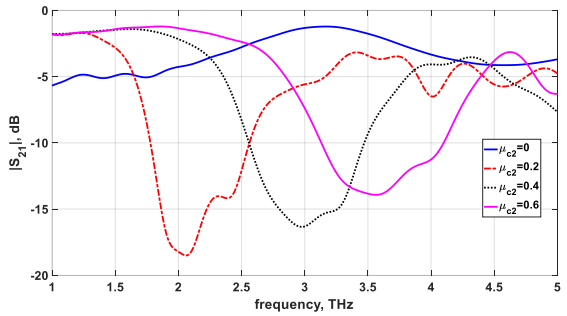

Fig. 2. Magnitude of S_{21} for the structure of Fig.1 with changing chemical potential of the middle graphene strip.

To provide an insight for the working principle and the reason of tunable response of the design of Fig. 1, electric field distribution is calculated and illustrated in Fig. 3, at the frequency of 3 THz and for the two cases of chemical potential of the middle graphene strip equal to $\mu_{c2} = 0\ eV$ and $\mu_{c2} = 0.4\ eV$. From Fig. 3(a), It is observed that for $\mu_{c2} = 0.4\ eV$ the propagating waves of the main transmission line are coupled to the beneath graphene strip and therefore, high insertion loss is resulted. The reason is that, when chemical potential of the middle graphene strip is $\mu_{c2} = 0.4\ eV$, graphene can support SPP waves with low loss and, due to low separation between the signal TL and the middle graphene strip, the propagating waves of the signal TL couples to the middle graphene strip and less energy is conveyed to the second port and high isolation is resulted.

However, when the chemical potential of the middle graphene strip is set as $\mu_{c2} = 0\ eV$, as shown in Fig. 3(b), the electromagnetic waves are mainly propagated on the main transmission line and guided to the output port because, in this case, the middle graphene strip can't support SPP waves.

B. Three longitudinal graphene strips in the substrate

To achieve more flexibility and cover broader application areas, three graphene ribbons, with equal lengths of $L = 18\mu m$, are included longitudinally under the main transmission line and in the substrate, as shown in Fig. 4. The width of the middle ribbon is $m = 5\ \mu m$ and the widths of the other two ribbons are equal to 2.4 μm. There is a gap of $g = 0.1\ \mu m$ between the ribbons. To better showcase the proposed design, the gaps are plotted larger than the real values. The ribbons are numbered as shown in Fig. 4. Chemical potentials of the longitudinal strips are designated by μ_{c1}, μ_{c2}, μ_{c3}, while chemical potential of the signal transmission line and the ground plane are characterized by μ_{c0}.

In the first step, the chemical potential of the main transmission line and the ground plane, represented by μ_{c0}, is assigned the two values of $\mu_{c0} = 1.4\ eV$ and $\mu_{c0} = 0.7\ eV$, and the chemical potentials of the middle graphene elements are assigned the two values of 0 eV and 1.4 eV and transmission of the structure is simulated and plotted in Fig. 5(a). It is observed that the proposed structure can be used as a tunable band-stop filter. Performance of the structure as a tunable band-stop filter, as shown in Fig. 5(a), illustrates that in the frequency range 0.1-7 THz, the 10 dB rejection band can be tuned to the bandwidths of 1.94-2.49 THz, 3.52-3.68 THz and 4.25-4.82 THz, depending on the chemical potentials of the graphene strips.

In the second step, assigning the chemical potential of all the graphene parts to three different values of 0 eV, 0.7 eV, and 1.4 eV, various states of transmission magnitudes are achieved, which makes the designed structure of Fig. 4 work as an amplitude modulator. To evaluate amplitude modulators, modulation depth, defined as follows, is considered [7]:

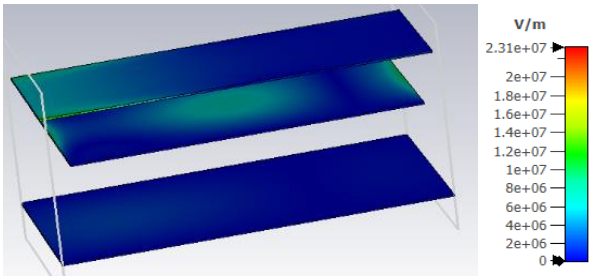

(a)

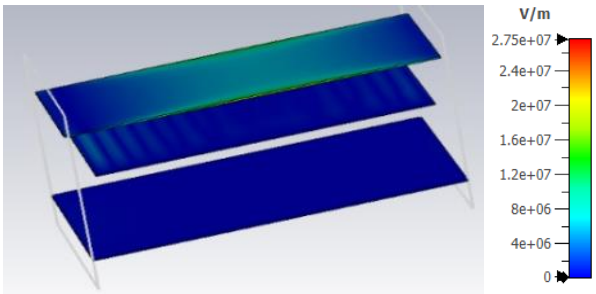

(b)

Fig. 3. Electric field distribution at 3 THz: (a) $\mu_{c2} = 0.4\ eV$, (b) $\mu_{c2} = 0\ eV$.

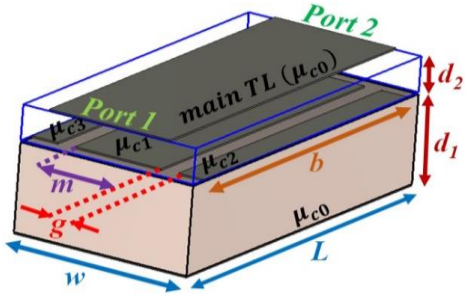

Fig. 4. Loaded substrate with three longitudinal graphene ribbons.

$$MD = \left(1 - \frac{T}{T_{max}}\right) \times 100 \quad (3)$$

Where, T represents transmission and T_{max} stands for maximum transmission of the structure. Modulation depth is calculated and plotted in Fig. 5(b). It is observed that at the frequency range of 3.4-3.8 THz, several discrete values of modulation depth with changing chemical potential of the graphene parts are obtained. The designed structure is quite efficient as an amplitude modulator and provides a maximum modulation depth of 100% with best performance at 3.6 THz. The performance of the proposed design in this paper is compared with the previously published series structures in the THz frequency band in Table II. As it is observed from the table, the proposed structure of this paper provides two different applications using the same structure.

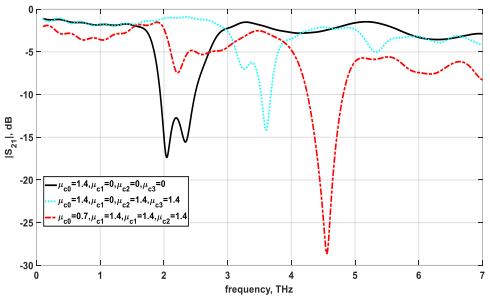

(a)

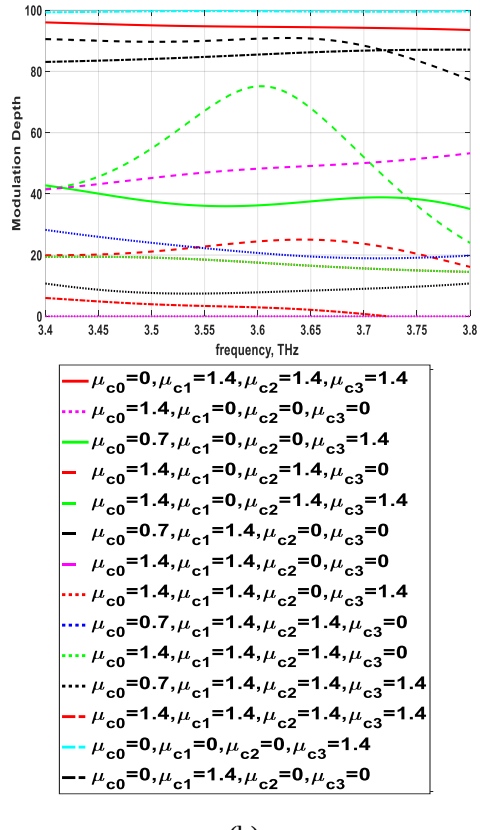

(b)

Fig. 5. (a) Transmission magnitude of the structure of Fig. 4 for three sets of chemical potentials, (b) modulation depth of the structure of Fig. 4 with changing chemical potential of all the graphene strips.

TABLE II
Comparison With Series Structures at the THz Frequency Band

Reference	Number of layers	Application	Frequency band
[1]	1	Switch	25-30 THz
[28]	2	Amplitude modulator	3.4-3.8 THz
This work	2	Tunable band-stop filter, Amplitude modulator	1.9-4.7 THz, 3.6 THz

IV. Conclusion

A layered series transmission line is introduced, the main conductor and the ground plane are implemented by graphene, and the dielectric is loaded by longitudinal graphene strips. It is shown that inserting a graphene strip in the substrate and changing its chemical potential in the range of 0-0.6 eV, provides a tunable band-stop filter with 10 dB rejection bands of 1.77-2.55 THz (36.1%), 2.55-3.47 THz (30.5%) and 3.13-4.1 THz (26.8%) with an all-pass response in 1-5 THz frequency band. With increasing the number of middle graphene strips to three and applying different chemical potentials to the graphene elements, both a tunable band-stop filter with reduced bandwidths of 1.94-2.49THz (24.8%), 3.52-3.68THz (4.4%), 4.25-4.82THz (12.56%), which is appropriate for high quality applications, and an amplitude modulator in the frequency band of 3.4-3.8 THz with optimum performance at the frequency of 3.6 THz and providing more than 10 cases of modulation depths from 0-100% are obtained.

Declaration of Competing Interest

The author declares that they have no known competing financial interests or personal relationships that could have appeared to influence the work reported in this paper.

Funding

No funding was received for this research.

Data availability

Data will be made available on request.

References

[1] J.-S. Gómez-Díaz and J. Perruisseau-Carrier, "Graphene-based plasmonic switches at near infrared frequencies," *Optics Express*, vol. 21, no. 13, pp. 15490-15504, 2013.

[2] I. Al-Naib, "Biomedical sensing with conductively coupled terahertz metamaterial resonators," *IEEE Journal of Selected Topics in Quantum Electronics*, vol. 23, no. 4, pp. 1-5, 2016.

[3] P. Zamzam, P. Rezaei, S. A. Khatami and Z. Mousavirazi, "Convertible Perfect Absorber with Single Ring Resonator: Tunable Single Band/Dual-Band Visible," *Modeling and Simulation in Electrical and Electronics Engineering*, vol. 1, no. 4, pp. 7-13, 2022.

[4] M. Ghaderi and P. Rezaei, "Wide Band THz Transmitarray Antenna Based on Graphene Slotted Lattice," *Modeling and*

Simulation in Electrical and Electronics Engineering, pp. 1-8, 2025.

[5] M. PourHosseini, S. Jarchi, P. Rezaei, and Z. Ghattan Kashani, "High gain multi-band circularly polarized bi-layered metasurface patch array antenna with dual-orthogonal feeds," *Optical and Quantum Electronics*, vol. 57, no. 2, p. 155, 2025.

[6] M. PourHosseini, S. Jarchi, P. Rezaei, and Z. Ghattan Kashani, "Terahertz microstrip array antenna with metasurface polarization conversion using silicon dioxide as dielectric layer," *Optical and Quantum Electronics*, vol. 56, no. 5, p. 796, 2024.

[7] Q. Zheng, L. Xia, L. Tang, C. Du and H. Cui, "Low voltage graphene-based amplitude modulator for high efficiency terahertz modulation," *Nanomaterials*, vol. 10, no. 3, p. 585, 2020.

[8] Y. Yao, X. Cheng, S.-W. Qu, J. Yu and X. Chen, "Graphene-metal based tunable band-pass filters in the terahertz band," *IET Microwaves, Antennas & Propagation*, vol. 10, no. 14, pp. 1570-1575, 2016.

[9] A. Shubham, D. Samantaray, S. K. Ghosh, S. Dwivedi, and S. Bhattacharyya, "Performance Improvement of a Graphene Patch Antenna using Metasurface for THz Applications," *Optik*, vol. 264, p. 169412, 2022.

[10] S. Armaghani, S. Khani and M. Danaie, "Design of all-optical graphene switches based on a Mach-Zehnder interferometer employing optical Kerr effect," *Superlattices and Microstructures*, vol. 135, p. 106244, 2019.

[11] M. Yaghobi, R. Rezaei and M. M. Fakharian, "Graphene-Based Planar Microstrip Patch Antenna with Circular Polarization Capability," *Modeling and Simulation in Electrical and Electronics Engineering*, vol. 1, no. 3, pp. 41-45, 2021.

[12] C. Casiraghi, A. Hartschuh, E. Lidorikis, H. Qian, H. Harutyunyan, T. Gokus, K. S. Novoselov and A. C. Ferrari, "Rayleigh imaging of graphene and graphene layers," *Nano letters*, vol. 7, no. 9, pp. 2711-2717, 2007.

[13] A. Adetayo and D. Runsewe, "Synthesis and fabrication of graphene and graphene oxide: a review," *Open Journal of Composite Materials*, vol. 9, no. 02, p. 207, 2019.

[14] D. Correas-Serrano, J. S. Gomez-Diaz, J. Perruisseau-Carrier, and A. Alvarez-Melcon, "Graphene-based plasmonic tunable low-pass filters in the terahertz band," *IEEE Transactions on Nanotechnology*, vol. 13, no. 6, pp. 1145-1153, 2014.

[15] H. Deng, Y. Yan, and Y. Xu, "Tunable flat-top bandpass filter based on coupled resonators on a graphene sheet," *IEEE Photonics Technology Letters*, vol. 27, no. 11, pp. 1161-1164, 2015.

[16] R. Emadi, A. Amirhosseini, M. Karimi, R. Safian, and A. Z. Nezhad, "Design of low-loss waveguide switch using graphene strips at THz frequencies," in *2016 Fourth International Conference on Millimeter-Wave and Terahertz Technologies (MMWaTT)*, 2016.

[17] Y. Zhang, Y. Feng, B. Zhu, J. Zhao, and T. Jiang, "Graphene-based tunable metamaterial absorber and polarization modulation in terahertz frequency," *Optics Express*, vol. 22, no. 19, p. 2274322752, 2014.

[18] N. Kakenov, M. S. Ergoktas, O. Balci, and C. Kocabas, "Graphene-based terahertz phase modulators," *2D Materials*, vol. 5, no. 3, p. 035018, 2018.

[19] Y. Feng, Y. Liu, X. Wang, D. Dong, Y. Shi and L. Tang, "Tunable multichannel plasmonic filter based on a single graphene sheet on a Fibonacci quasiperiodic structure," *Plasmonics*, vol. 13, no. 2, pp. 653-659, 2018.

[20] E. Shokati, S. Asgari and N. Granpayeh, "Dual-band polarization-sensitive graphene chiral metasurface and its application as a refractive index sensor," IEEE *Sensors Journal*, vol. 19, no. 21, pp. 9991-9996, 2019.

[21] N. Kiani, F. T. Hamedani and P. Rezaei, "Designing of a circularly polarized reconfigurable graphene-based THz patch antenna with cross-shaped slot," *Optical and Quantum Electronics*, vol. 55, no. 4, p. 356, 2023.

[22] B. Khodadadi, P. Rezaei and S. Hadipour, "Accurate graphene-based absorber for slight leakage detection of Radon and chloroform air-pollution," *Results in Physics*, vol. 71, p. 108196, 2025.

[23] S. E. Hosseininejad, K. Rouhi, F. Wang, M. Khalily and R. Tafazolli, "High-speed terahertz communication with graphene-based time-modulated low-bit phase coding metasurfaces: A novel architecture for enhanced performance," *Materials Today Communications*, vol. 40, p. 109726, 2024.

[24] I. Marasco, C. Cantore, G. V. Bianco, G. Bruno, A. D'orazio, and G. Magno, "Transparent Graphene-Based RIS for 6G Communications in the THz Spectrum," *IEEE Open Journal of Antennas and Propagation*, 2024.

[25] J. Muheki, J. Wekalao, H. B. Albargi, M. Jalalah, A. H. Almawgani, and S. K. Patel, "A graphene gold metasurface inspired surface plasmon resonance sensor designed for terahertz applications in sensing and detection of heavy metals in water," *Plasmonics*, vol. 20, no. 1, pp. 289-303, 2025.

[26] S. Khani, "Compact and Tunable Microstrip Bandpass Filter Using a Disk Resonator and a U-shaped Waveguide for Wi-MAX and WLAN Applications," *Modeling and Simulation in Electrical and Electronics Engineering*, vol. 3, no. 2, pp. 29-35, 2023.

[27] A. Parsa, P. Rezaei, A. Amne Elahi, and Z. Mousavirazi, "High-Efficiency Slot Array Antenna Fed by a Microstrip Line to ESIW Transition for X-band Applications," *Modeling and Simulation in Electrical and Electronics Engineering*, vol. 3, no. 1, pp. 47-52, 2023.

[28] S. Jarchi, "Amplitude Modulator Design Using Series Graphene Transmission Lines in Terahertz Frequency Band," *IEEE Transactions on Nanotechnology*, vol. 23, pp. 323-328, 2024.

[29] M. Mokhayer, S. Jarchi and R. Faraji-Dana, "Multifunctional reconfigurable metasurfaces for manipulation of transmitted wave in THz Band," *Optical and Quantum Electronics*, vol. 56, no. 6, p. 1038, 2024.

[30] M. Mokhayer, S. Jarchi and R. Faraji-Dana, "Miniaturized meandered ring graphene-metal metasurface with wide angle control on the transmitted wave," *AEU-International Journal of Electronics and Communications*, vol. 187, p. 155566, 2024.